Ljubica Milović [1], Vesna Milošević-Mitić [2], Zoran Radaković [2], Nina Anđelić [2], Blagoj Petrovski [3]

ASSESSMENT OF PRESSURE VESSEL LOAD CAPACITY IN THE PRESENCE OF CRACKS

PROCENA NOSIVOSTI POSUDE POD PRITISKOM U PRISUSTVU PRSLINE

Originalni naučni rad / Original scientific paper
UDK /UDC: 620.172.24: 66-988
Rad primljen / Paper received: 18.03.2013.

Adresa autora / Author's address:
1) University of Belgrade, Faculty of Technology and Metallurgy, Belgrade, Serbia, acibulj@tmf.bg.ac.rs
2) University of Belgrade, Faculty of Mechanical Engineering, Belgrade, Serbia
3) University of Belgrade, Faculty of Mechanical Engineering – Innovation Centre, Belgrade, Serbia

Keywords
- J-integral
- crack driving force
- resistance curve
- pressure vessel

Ključne reči
- J-integral
- sila rasta prsline
- kriva otpornosti
- posuda pod pritiskom

Abstract

The paper illustrates the structural assessment of an investigated pressure vessel, made of low-alloyed high strength steel, with an external surface crack located on the shell wall. In order to assess the remaining strength and the resistance to stable crack growth, the J-integral is experimentally measured at operating temperature of –40°C. The compared crack driving force and material resistance to crack growth have determined the size of the zone of stable crack development, as well as the critical crack length. Also given is the pressure vessel calculation code by applying the theory of finite elements to linear-elastic material behaviour. Critical pressure values are calculated by analytical and numerical procedures and show good agreement.

Izvod

U radu je prikazana ocena integriteta ispitne posude pod pritiskom izrađene od niskolegiranog čelika povišene čvrstoće sa spoljašnjom površinskom prslinom na zidu omotača. Da bi se ocenila preostala čvrstoća i otpornost na stabilan rast prsline, eksperimentalno je izmeren J-integral na radnoj temperaturi od –40°C. Poređenjem sile rasta prsline i otpornosti materijala na rast prsline određena je veličina zone stabilnog rasta prsline kao i kritična veličina prsline. Prikazan je i proračun posude pod pritiskom primenom teorije konačnih elemenata za linearno-elastično ponašanje materijala. Kritične vrednosti pritisaka izračunate analitičkim i numeričkim postupkom pokazuju dobro slaganje.

INTRODUCTION

Pressure vessels are fabricated in various geometrical forms (cylindrical, cone, spherical, or combined), volumes and sizes, and are used for different purposes.

Although high safety factor values are implemented in the design of pressure vessels, the insufficient knowledge of operating conditions and how they change, and the poor quality control in fabrication, diminish the pre-designed safety factor to a large extent. The assessment of pressure vessel safety and the risk in exploitation includes the consideration of implications of leak-before-break and total collapse due to brittle fracture.

Cracks in components exposed to static and variable loads grow in a stable manner to a certain period (subcritically) and may develop as instable – critical, depending on the operating conditions. The analysis of the behaviour of pressure vessels exposed to internal pressure is aimed in assessing the structural limit load capacity when the structure contains crack-like defects. Assessment of detected or assumed defects safety, i.e. the assessment on whether defects will become critical within the observed operation period, the so-called conservative assessment, is based on linear elastic (LEFM)- or elastic-plastic (EPFM) fracture mechanics.

Pressure vessels considered are defined as stationary vessels used for liquefied gas storage under pressure, made of NIONIKRAL 70 (NN 70) produced by Ironworks Jesenice, low-alloyed high strength steel (HSLA), specified for operating temperatures ranging from –40 °C to ambient temperature. These vessels are usually components of pressure equipment in the processing-, petro-chemical and oil industries.

SAFE OPERATION AND DESIGN PROBLEMS

The design and fabrication of pressure equipment strict conforms regulations and codes, to the aim to assure the required safety during the expected exploitation period. Technical regulations for calculating pressure vessels are aimed at defining the difference between the operating pressure and one or more characteristic pressures that may lead to fracture. Pressure vessels and pipelines are mostly designed for an operating life from 10 to 25 years, and because of the devastating effects that can occur at structural failure – catastrophic failure, the investors do not allow the operation of a component having a detected crack, thus emphasizing the efforts for devoting much attention to the problem of assuring the integrity of the pressure vessel.

The concept of leak-before-break (LBB) is a widely accepted method for determining the pressure components' susceptibility to fracture, due to the stable development of cracks. Because of the fatigue loading and/or stress corrosion, the initial crack in the pressure vessel wall tends to grow through the thickness in a stable manner and ruptures the wall of the vessel and so the fluid begins to leak. The leak that precedes the global failure of the component is easily noticeable, and so the local wall through-thickness fracture is considered controlled. In the mid 20th century, Irwin had suggested adopting the leak-before-break criterion for designing pressure vessels /1-6/.

Alternatively, the surface crack can lead to catastrophic failure with an absence of leakage. The possibility for a sudden and unexpected brittle fracture is an important problem in the safety analysis and risk of failure assessment of pressure components. Brittle fracture occurs when the crack or defect experiences high stresses and low toughness of the material. In fact, the initial defect can remain undetected, and high stress values may result from a geometrical stress concentration or from residual stresses, often created in the welding process. Material toughness is a measure of the susceptibility of materials to brittle fracture and it decreases at low temperature.

Proof pressure testing is obligatory before putting pressure vessels into service. Overpressure values required for testing have been the matter of debate in the scientific and professional community, since overpressure must not be the cause of a functional damage and result in the decrease of the safety of the component. At least 200 times higher deformation energy is released in the air than in water for the same overpressure which must be accounted for when performing air pressure tests. Conditions of brittle fracture (low temperature operation, non heat-treated welded joints, incomplete inspection and low material toughness) give an explanation to why this type of fracture sometime occurs after the hydro test: – when the fluid operating temperature is much lower than the hydro test temperature; cracks created during the pressure test may develop in exploitation and if they cannot be detected, failure is most certain.

Pressure tests up to explosive fracture are applied in exceptional cases since they are costly and demanding. The aim of this test is to determine the degree of plasticity of the vessel or pipe, defined by the percentual plastic deformation at fracture.

HISTORICAL BACKGROUND

Since 1828, the French *Conseil général des mines* has adopted a relation between the pressure responsible for vessel fracture and the ultimate tensile strength of the material used for determining the boiler wall thickness /3/ as:

$$t = 9\frac{pR_i}{\sigma'_M} + 3 \tag{1}$$

In Eq.(1) $t = R_0 - R_i$ is the wall thickness, where R_0 and R_i are the external and internal radii of the cylindrical boiler shell, p is operating pressure, while 9 is the safety factor, and 3 mm is a thickness correction due to corrosion. σ'_M is the value of ultimate strength, with a limit up to 260 MPa. The hydro test has required a pressure 3 times higher than the operating pressure.

In 1911, while performing experiments on pressure vessels, Cook and Robertson noticed that cylindrical vessels made of soft steel deform at the diameter along with the increasing pressure, slowly at first, then rapidly, and finally they bulge before cracking. They had observed that the "highest pressure in the cylinder was larger than the pressure at the instant of fracture, owing to the fast dilatations that had preceded" /3/.

For ideal plastic materials that do not strengthen by deformation, in the region of small deformations, with sufficient accuracy, the tensile properties are known not to exhibit any changes with the increasing deformation. When plastic deformation starts, at first it is limited to the material that is in the zone of elasticity until plasticity is reached throughout the thickness, or a *plastic joint* develops. This type of load is the *threshold*, above which the structure cannot resist deformations if material behaviour remains plastic. When deformations overcome those at threshold loads, most materials tend to strengthen by deformation which is manifested in the increase of tensile properties. The internal pressure in vessels increases the material tensile properties, and the stress increases as a result of the reduction of the net section. As a result of these two processes, a maximal resisting pressure develops in the cylinder. This phenomena is called *plastic instability*, and does not represent the fracture but it advances rapidly to fracture with a persisting load.

Early pressure vessel design required the determination of the safety factor with respect to fracture, due from the increased pressure for plastic instability. Later, the safety factor was associated with the onset of large deformations, or the limited pressure, that precedes the fracture. These two approaches have limited the allowable stresses to a fraction of the ultimate strength, or to the yield strength of the material. In certain countries, the safety factor with respect to the limiting pressure is considered as a sufficient criterion in the design, while elsewhere, two safety factors are applied: with respect to rupture pressure, and a sufficient deformation with values between the onset of large deformations and burst fracture.

EXPERIMENTS

A procedure is considered for the limit load assessment of the remaining ligament in a cylindrical wall of a test vessel with a initial crack as shown in Fig. 1. The crack is located on the outer vessel wall surface, of length $2a$ = 108 mm and initial depth d_0 = 5 mm. The vessel is used for the storage of liquefied gas under pressure. The shown prototype is fabricated by welding NN 70 steel of nominal yield strength $R_{p0.2}$ = 780 MPa, ultimate strength R_m = 820 MPa (Table 1), with chemical contents given in Table 2.

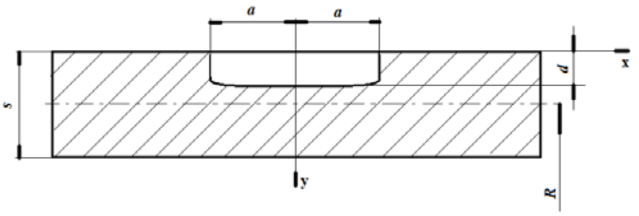

Figure 1. Shell geometry with an outer surface crack of length 2*a* and depth *d*
Slika 1. Geometrija ljuske sa spoljnom površinskom prslinom dužine 2*a* i dubine *d*

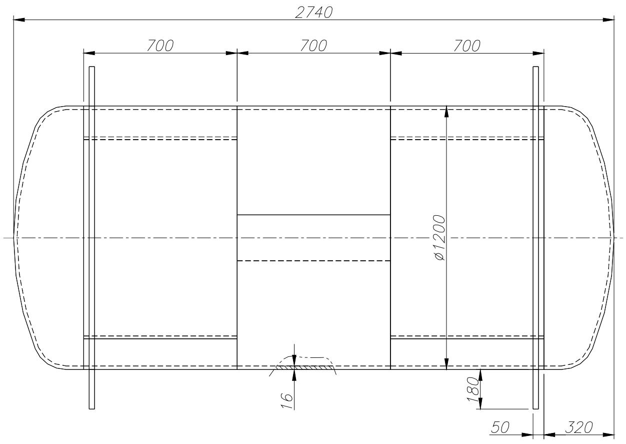

Figure 2. Test pressure vessel for liquefied gas storage.
Slika 1. Ispitna posuda pod pritiskom za skladištenje utečnjenih gasova

Table 1. Physical and tensile properties of parent- and weld metal.
Tabela 1. Fizičke i zatezne karakteristike osnovnog i metala šava

Material	*Young modulus* E, GPa	*0,2% proof strength* $R_{p0.2}$, MPa	*Ultimate strength* R_m, MPa	*Poisson's ratio* ν	Coefficient of thermal expansion α, 1/°C
NN 70-PM	199	780	820	1/3	$12\text{x}10^{-6}$
WM	/	718	791	1/3	/

Table 2. Chemical composition of pressure vessel material, % wt.
Tabela 2. Hemijski sastav materijala posude pod pritiskom, % tež.

C	Si	Mn	P	S	Cr	Ni	Cu
0.106	0.209	0.220	0.005	0.0172	1.2575	2.361	0.246
Al	Mo	Ti	As	V	Nb	Sn	Ca
0.007	0.305	0.002	0.017	0.052	0.007	0.014	0.0003
B	Pb	W	Sb	Ta	Co	N	
0	0.0009	0.0109	0.007	0.0009	0.0189	0.0096	

Table 3. Geometrical measurements of the vessel and surface crack in the shell wall.
Tabela 3. Geometrijske mere posude i površinske prsline na njenom omotaču

mean radius of cylindrical shell	R, mm	592
length of cylindrical shell	L, mm	2100
wall thickness of cylindrical shell	s, mm	16
surface crack size (length × depth)	($2a \times$ d), mm	108 × 5
ratio of surface crack depth to vessel wall thickness	d/h, mm	0.312
shell parameter	λ	1

The vessel is produced as a one-piece, stationary, horizontal, with torispherical heads welded to the cylindrical shell by shielded metal arc welding (SMAW) of segments 700 mm in length. The outer diameter of the vessel is D_s = 1200 mm, and wall thickness s = 16 mm. Table 3 shows the geometrical measurements of the tested vessel and the investigated surface crack. The operating temperature in the vessel is $t = -40$°C.

According to design, the allowable stress is calculated as the lesser of the two quotients:

$$\sigma_{zdoz} = \min\left\{\frac{R_{p0.2}}{1.5};\frac{R_m}{2.4}\right\} = 342 \text{ MPa}$$

The allowable operating pressure for the vessel shell with no defects is determined based on the boiler formula and equals $p_{allow.}$ = 9.243 MPa = 92.43 bar, with a weld factor φ = 1 and corrosion correction c = 0. The longitudinal stress is σ_x = 342 MPa and it is twice the value of the circumferential stress σ_z = 170.94 MPa.

Thermal stresses in the pressure vessel wall /4, 7/ are calculated in the case of outer surface shell temperature t_1 = 40°C, inner surface temperature t_2 = –40°C, with the assumption of linear change in temperature through wall thickness, according to Eq.(2):

$$\sigma_x = \sigma_\phi = \pm\frac{E\alpha(t_1 - t_2)}{2(1-\nu)}, \tag{2}$$

and are $\sigma_x = \sigma_\varphi = \pm143.28$ MPa, where the '+' sign refers to the outer surface with tensile stress if $t_1 > t_2$.

The crack opening mode of fracture, known as mode I, defined as the separation of fractured surfaces by tensile stress symmetrical to the initial crack plane /8/, is a characteristic of axial surface cracks in vessels or pipes exposed to internal pressure. For this case the critical value of the stress intensity factor K_{Ic} or plane strain fracture toughness, is calculated as:

$$K_{Ic} = \sigma_c\sqrt{\pi a}, \tag{3}$$

where fracture occurs at stress σ_c in a specimen with crack length a. Apparently, the plane stress state is dominant for the investigated thin-walled pressure vessel, because of the ratio s/D = 0.0135 and material properties. Hence, the fracture mechanics parameter *COD* (crack opening displacement) is used for the vessel limit load assessment, since it includes a more pronounced plastic behaviour. The COD is directly proportional to the *J*-integral that may be used, as its critical value J_{Ic}, for determining K_{Ic} on samples that are not required to fracture in conditions of plane strain.

REMAINING STRENGTH ASSESSMENT BY *R*-CURVE

During the 60s, Irwin, Krafft, et al., /9, 10/, have introduced the fracture criterion based on material resistance to crack growth. According to this criterion the crack grows in a stable manner as long as the increase in *resistance to crack growth*, *R*, is greater than the increase of the acting stress intensity factor *K*, or

$$\frac{\partial R}{\partial a} > \frac{\partial K}{\partial a} \tag{4}$$

Fast fracture develops when

$$K = R \text{ and } \frac{\partial K}{\partial a} > \frac{\partial R}{\partial a} \qquad (5)$$

In order to include the influence of plasticity, this concept can be extended to the use of the J-integral instead of the stress intensity factor K.

The remaining load capacity of the structure in the presence of a crack can be determined when the following is known, /11/:

– $\sqrt{J_R}$ material curve for the material of the structure, from testing samples;
– J-integral value for the tested structure at various crack lengths and acting loads/stresses by applying a suitable plasticity model in front of the crack tip and from plotted $\sqrt{J}$ -curve graphs, and
– point of instability from $\sqrt{J}$ -curves and $\sqrt{J_R}$ -material curves of the structure.

In this paper, the limit load assessment of the pressure vessel in the presence of a crack is based on the J-integral that may be applied to a certain degree as a unique fracture mechanics parameter in the elastic region and even after the plasticity limit has been reached. The case of a thin-walled cylindrical shell of parameter $\lambda = 1$ with a longitudinal external surface crack has also been investigated.

The necessary data for limit load capacity assessment is the material resistance curve for crack growth (J–Δa or J_R-curve), where Δa is crack extension. Tests are performed at the Bay-Logi Institute for Logistics and Production Systems, at Miskolctapolca, Hungary, in the low temperature chamber, using a servo-hydraulic INSTRON 8803 machine with the compliance method that gives average values of the crack length. The testing temperature was –40°C.

Three-point bend specimens, shown in Fig. 3, with introduced fatigue pre-cracks were loaded by constantly increasing bending forces and were successively unloaded as shown in the diagram *load*–CMOD (crack mouth opening displacement), Fig. 4.

From the contributing compliance and from the slope of the unloading curve, an instantaneous crack length is determined for all calculated J-integral values, that is necessary for plotting the J_R–curve, Fig.5.

At the intersection of the J_R-curve and the crack tip blunting line given by Eq.(6):

$$J = 2\bar{\sigma} \cdot \Delta a \,, \qquad (6)$$

the value J_{Ic} = 341.8 N/mm is calculated, and the fictive crack propagation value from the crack blunting Δa = 0.214 mm. Here, $\bar{\sigma}$ is the mean plastic strengthening stress of the specimen, calculated from Eq.(7):

$$\bar{\sigma} = \frac{R_{p0.2} + R_m}{2} \qquad (7)$$

Calculated values make the basic initial data on the behaviour of the tested NN 70 material in the presence of a crack. In order to apply these values to the investigated pressure vessel structure, it is necessary to plot the *crack driving force* (CDF) curves for the shell structure, assumed as a cylindrical shell, /7, 12-15/. The CDF curves, representing the J-integral dependence on crack extension at a constant value of the load (stress), are determined by the shell parameter λ:

$$\lambda = \left[12(1-\nu^2)\right]^{1/4} \frac{a}{\sqrt{Rs}} \,, \qquad (8)$$

where, a is the half length of the outer surface crack, Fig. 1. From Eq.(8), the proportionality is evident between the crack half length a and shell parameter λ.

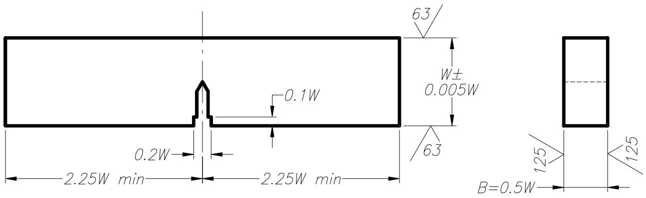

Figure 3. Three-point bend specimen
Slika 3. Epruveta za savijanje u tri tačke

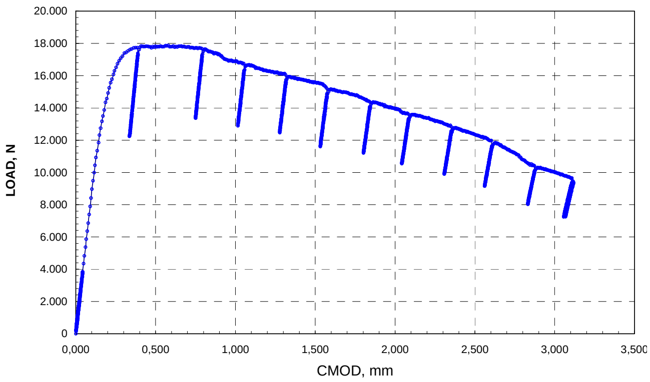

Figure 4. Load–CMOD diagram for determining the J-integral
Slika 4. Dijagram sila-CMOD za određivanje J-integrala

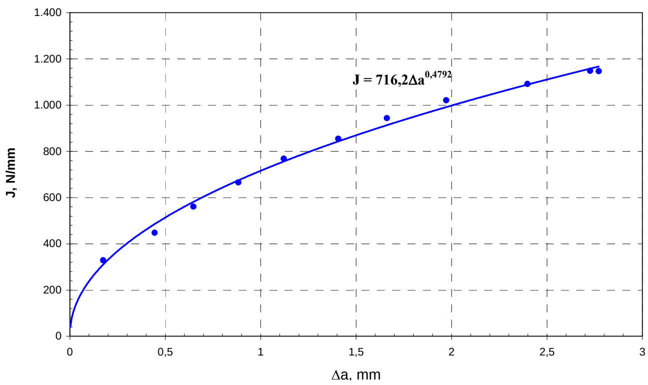

Figure 5. Resistance curve J–Δa.
Slika 5. Kriva otpornosti J-Δa

For the crack shown in Fig. 1, the relation holds:

$$J^* = \frac{JE}{4aR_{p0.2}^2} = \frac{2\sqrt{3}}{3}\left[\frac{\delta_0}{d_1} + \frac{\theta_2}{d_2}\left(0.5 - \frac{d}{s}\right)\right] \qquad (9)$$

where, J^* is the normalized value of J-integral, J is current value of J-integral, and d_1 and d_2 are determined from

$$d_1 = \frac{4aR_{p0.2}}{E} \text{ and } d_2 = \frac{4aR_{p0.2}}{sE} \qquad (10)$$

The values δ_0/d_1 and θ_2/d_2 depend on the shell parameter λ and on the fraction of crack depth d/s, /12, 14/.

The plot in Fig. 6 shows the change of $\sqrt{J^*}$ for shell parameter $\lambda = 1$ with fraction of crack depth d/s at constant values of $(pr/sR_{p0.2})$ and $J_R^{0.5}$ for the resistance curve of the specimen made of parent metal and transferred from Fig. 5, with an initial crack depth of $d_0 = 5$ mm.

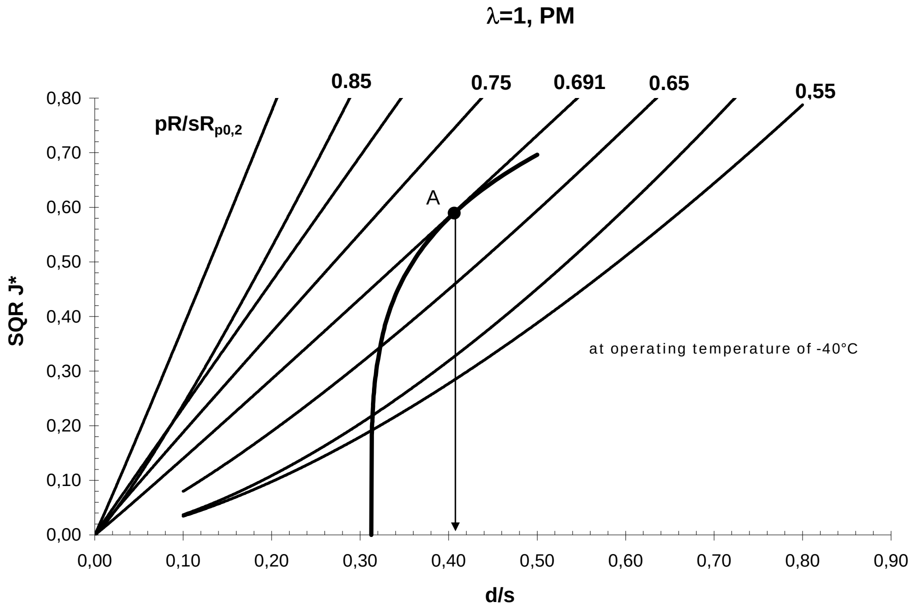

Figure 6. Limit load assessment diagram for the cylindrical pressure vessel with an axial crack.
Slika 6. Dijagram za procenu nosivosti cilindrične posude pod pritiskom sa aksijalnom prslinom

DISCUSSION

A crack length of $2a = 108$ mm is calculated from Eq.(8) and for shell parameter $\lambda = 1$. Plots on the diagram in Fig. 6 show that for the surface crack of initial depth $d_0 = 5$ mm and length $2a = 108$ mm, the common tangent on the CDF curve gives $(pr/sR_{p0.2}) = 0.691$. The remaining load carrying ligament at initial crack depth d_0 equals

$$b_0 = s - d_0 = 16 - 5 = 11 \text{ mm}.$$

The crack shall continue to grow in a stable manner in the plastic zone up to the point of instability A, whose coordinates are (0.406; 0.5895), so that up to the depth of

$$d \le s\cdot 0.406 = 16\cdot 0.406 = 6.496 \text{ mm}$$

there is no risk of fast fracture. The limit pressure of the vessel with a 6.4 mm crack depth is then

$$p = 0.691\frac{16\cdot 780}{592} = 14.567 \text{ MPa} = 145.67 \text{ bar},$$

$$p > p_{allow.} = 92.43 \text{ bar},$$

$$p > p_i = 120.16 \text{ bar}.$$

This pressure value is higher than the calculated values of the operating and testing pressures for a vessel having no defects in the shell. The remaining ligament at the length of 108 mm is then

$$b = s - d = 16 - 6.496 = 9.504 \text{ mm}.$$

PRESSURE VESSEL CALCULATION BY APPLYING THE LINEAR FINITE ELEMENT THEORY

The first calculation model is formed based on 751 nodal points that define 708 plate finite elements. The model is presented in Fig. 7 with appropriate boundary conditions. The calculation is done for one quarter of the pressure-vessel, using the program package KOMIPS /16, 17/.

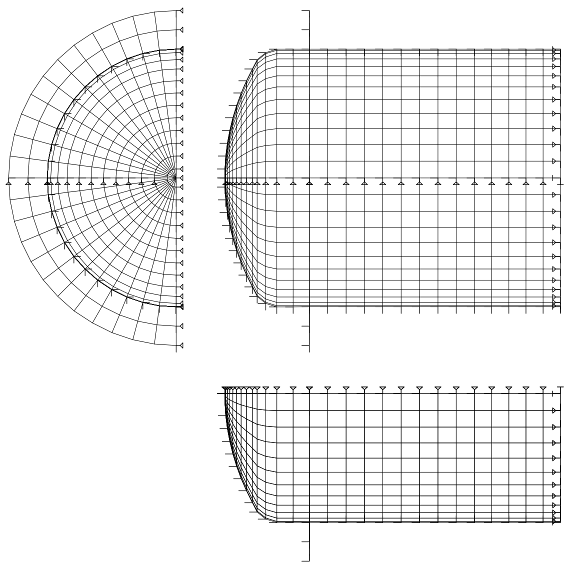
Figure 7. The FEM model and supports.
Slika 7. MKE model, oslonci

Three cases of the loading are investigated: the first (I) case represents a steady internal pressure of 100 bar, the second (II) case of loading is thermal loading, and the third (III) case represents their combination. In the II case, a temperature of –40°C is taken at the inner surface of the vessel, and +40°C for the outer surface. In order to simulate this loading, the plates are assumed to be at a mean temperature of 0°C, the ambient temperature is 40°C and the gradient of temperature change across the plate thickness is 5 °C/mm. The influence of dead weight of the structure is negligible. Figure 8 shows the deformed vessel under pressure for loading cases I and II.

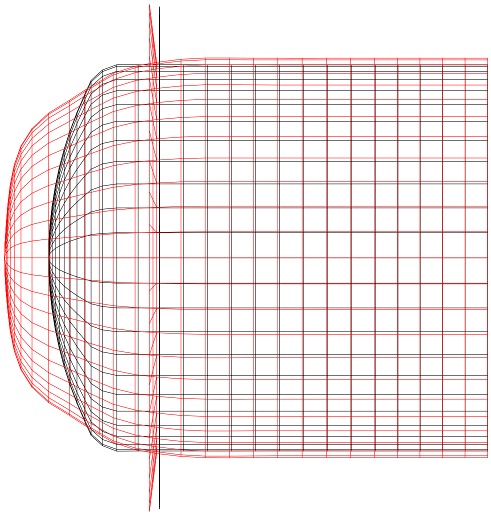

I loading case - internal pressure

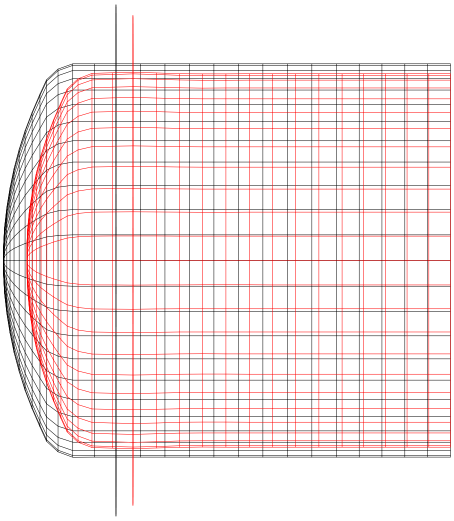

II loading case - thermal

Figure 8. Deformations for loading cases I and II.
Slika 8. Deformacija pri I i II slučaju opterećenja

The maximal calculated deformation in the case of internal pressure of 100 bar is 7.05 mm, and 0.75 mm in the second case, Fig. 8. As deformation fields in these cases have opposite directions, in the third loading case, the total maximal calculated deformation is 6.61 mm.

The equivalent stress is calculated by using the Huber-Hancky-Mises hypothesis. The obtained results are presented in Fig. 9. In all loading cases the maximal stresses act in the toroidal part of the head. Values determined are: in the first loading case 913 MPa; in the second 142 MPa; and in the third case 890 MPa. The weakest part of the vessel is the toroidal section of the head.

The linear finite element method has been applied in this calculation, where simple calculations have obtained allowable limit pressure loading values that are close to those calculated with the appropriate boiler formula.

The influence of the crack located in the cylindrical shell is investigated, and thus the equivalent stresses for this model are: 324 MPa (I loading case), 137 MPa (II loading case), and 448 MPa (III loading case). A comparative view of the obtained results is given in Table 4.

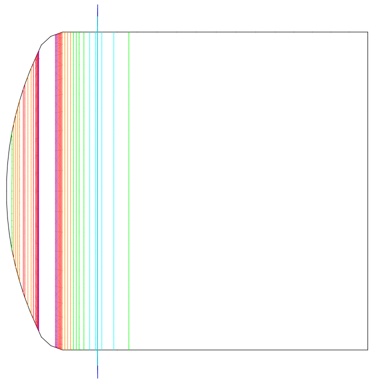

I case, internal pressure load

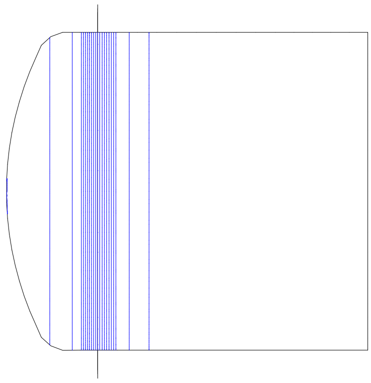

II case, thermal load

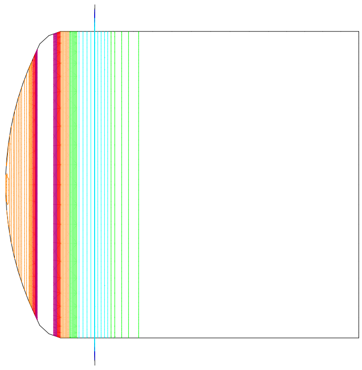

III case, internal pressure and thermal load

Equivalent stress, MPa
7.61E+02 ... 9.13E+02
6.09E+02 ... 7.61E+02
4.57E+02 ... 6.09E+02
3.04E+02 ... 4.57E+02
1.52E+02 ... 3.04E+02
0.00E+00 ... 1.52E+02

Figure 9. Equivalent stresses in the wall of the pressure vessel exposed to the I, II and III loading cases.
Slika 9. Ekvivalentni naponi u zidu posude pod pritiskom izložene dejstvu I, II i III slučaja opterećenja

Table 4. The obtained results
Tabela 4. Dobijeni rezultati

Loading case		Maximal deformation, mm	Maximal equivalent stresses, MPa	Equivalent stresses in the shell, MPa
I	Internal pressure 10 MPa	7.048	913	324
II	Thermal load –40 to +40°C	0.747	142	137
III	Combined loading	6.609	890	448

Individual stresses required for a detailed calculation at a pressure load of 100 bar are the longitudinal stress of 187 MPa, and circumferential stress of 374 MPa.

CRACK CALCULATION BY APPLYING THE LINEAR FEM THEORY

A detailed calculation of the crack influence, located in the cylindrical shell, required a new FEM model of 14495 nodal points. A part of the cylinder, 708 mm in length, is simulated with 10500 volume finite elements. The precise loading data input had required a generation of an 3800 element mesh, constituted by thin plate type elements, as shown in Fig. 10. The model does not include crack growth, so all calculated values relate to the configuration with the initial fatigue crack of the size $2a$ and d_0.

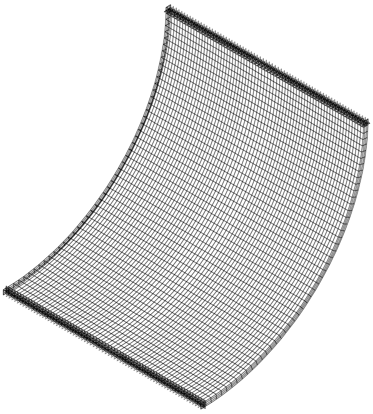

a) Plate finite elements and supports

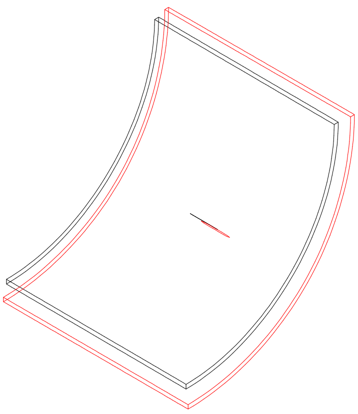

b) Contour deformations of volume finite elements (pressure load)

Figure 10. Shell segment model with crack
Slika 10. Model dela omotača sa prslinom

The three previously described loading cases are also considered for this model. In order to achieve the I case, a corresponding axial pressure of 187 MPa is added to the internal radial pressure of 10 MPa. The temperature range from –40 to +40°C is defined for all nodes depending on the radius.

The deformation field is similar for all three loading cases and is shown in Fig. 10b. The displacement of the shell in the first case is 1.27 mm (outer surface), and 0.29 mm (inner surface) in the second case, and finally 1.32 mm on the pressure side in the third case.

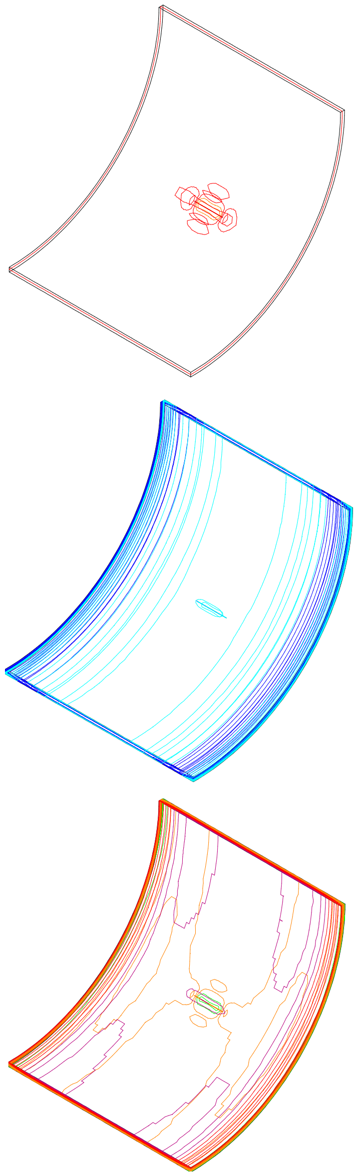

Equivalent stress, MPa

3.81E+02 ... 4.14E+02
3.05E+02 ... 3.81E+02
2.29E+02 ... 3.05E+02
1.52E+02 ... 2.29E+02
7.62E+01 ... 1.52E+02
6.00E-04 ... 7.62E+01

Figure 11. Stress fields for all three loading cases.
Slika 11. Naponsko polje za sva tri slučaja opterećenja

The crack influence can be defined based on the obtained stress fields. The stress in the I loading case is approximately constant throughout the shell thickness, the axial stress is 187 MPa and the radial stress is 361 MPa. Equivalent stresses for loading cases are shown in Fig. 11, while Fig. 12 shows the distribution of equivalent stresses in the vicinity of the crack. It is evident that a crack of 108 mm in length and 5 mm deep causes only a local stress concentration and does not substantially increase the stress concentration magnitude.

Temperature distribution is such that the stress increases on the inner surface of the vessel, and decreases on the outer surface that contains the crack. The maximal stress from thermal loading is 121 MPa. At a pressure of 10 MPa, the stress remains below 280 MPa at almost up to half of the shell thickness. In this way the previously concluded remark is confirmed: crack propagation is not likely at operating pressures and temperatures. At higher pressure values, the stress does not exceed the allowed value, and so the linear finite element theory is not capable of giving a precise calculation.

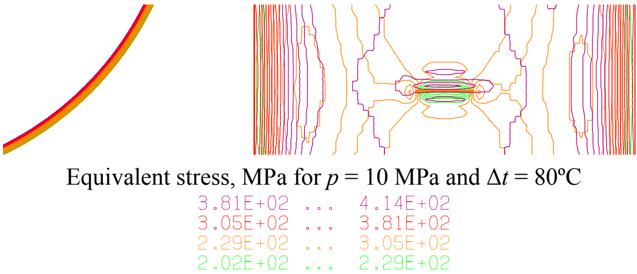

Figure 12. Equivalent stress distribution around the crack.
Slika 12. Raspodela ekvivalentnog napona oko prsline

CONCLUSION

The investigated pressure vessel in plane stress conditions with an outer surface crack of 5 mm depth located on the shell, can continue with operation even if the pressure jumps to 120.2 bar, as is the testing pressure. The safe operation of vessels of this type may be expected also for proportionally larger defects, since there is no risk of a leak-before-break, and no risk of catastrophic failure.

ACKNOWLEDGEMENTS

The research presented in this paper is accomplished through the financial support from the Ministry of Education, Science and Technological Development of the Republic of Serbia, project TR35011 grants. The authors particularly acknowledge Péter Rózsahegyi, the Head of the Department of Technical Risk Management at the Institute for Logistics and Production Systems of the Bay Zoltán Foundation for Applied Research, Miskolc, Hungary, who has helped us in the experiments, and our colleague Jovan Savić, dipl. ing. for the drafting used in this paper.

REFERENCES

1. Irwin, G.R., *Fracture of Pressure Vessels*, Materials for Muscles and Spacecraft, pp.204-229, McGraw Hill, 1961.
2. Irwin, G.R, Srawley, J.E., *Progress in the Development of Crack Toughness Fracture Tests*, Materialprufung, 1962, pp.1-11.
3. Labens, R., *Mehaničke osnove tehničkih propisa za proračun debljine zida sudova pod pritiskom. Primena na višeslojne sudove*, Monografija „Savremeni aspekti projektovanja i izrade sudova i cevovoda pod pritiskom“, pp.17-35, Institut Goša i TMF, 1982.
4. Moss, D.R., Pressure Vessel Design Manual, Elsevier, 2004.
5. Gubeljak, N., Predan, J., Kozak, D., *Leak-Before-Break Analysis of a Pressurizer - Estimation of the Elastic-Plastic Semi- elliptical Through-Wall Crack Opening Displacement*, Structural Integrity and Life, 12 (1), 2012, pp.31-34.
6. Jovičić, R., Sedmak, A., Sedmak, S., Milović, Lj., Jovičić, K., *Leakage of an Austenitic Steel CO_2 Storage Tank*, Structural Integrity and Life, 12 (2), 2012, pp.105-108.
7. Timošenko, S., Vojnovski-Kriger, S., Teorija ploča i ljuski, Građevinska knjiga, Beograd, 1962.
8. Sedmak, S., *Razvoj i osnovne definicije mehanike loma*, Monografija „Uvod u mehaniku loma i konstruisanje sa sigurnošću od loma“, pp.1-27, Institut Goša i TMF, 1980.
9. Irwin, G.R., *Fracture Testing of High Strength Sheet Materials Under Conditions Appropriate for Stress Analysis*, Report 5486, U.S. Naval Research Laboratory, July 27, 1960.
10. Krafft, J.M. et al., *Effect of Dimensions on Fast Fracture Instability of Notched Sheets*, Proceedings of the Crack Propagation Symposium, College of Aeronautics, Vol.1, Cranfield, England, 1961.
11. Ratwani, M.M., Sedmak, S., Petrovski, B., *Procena preostale čvrstoće sudova pod pritiskom sa površinskim greškama pomoću krive otpornosti*, Monografija „Mehanika loma zavarenih spojeva“, pp.131-163, Institut Goša i TMF, 1985.
12. Ratwani, M.M., *Koncept procurivanja pre loma kod sudova pod pritiskom*, Monografija „Savremeni aspekti projektovanja i izrade sudova i cevovoda pod pritiskom“, pp.79-91, Institut Goša i TMF, 1982.
13. Milović, Lj., Vuherer, T., Zrilić, M., Momčilović, D., Jaković, D., *Structural Integrity Assessment of Welded Pressure Vessel Produced of HSLA Steel*, Journal of Iron and Steel Research International, 18 (1-2), 2011, pp.888-892.
14. Ratwani, M.M, Erdogan, F., Irwin, G.R., *Fracture Propagation in Cylindrical Shell Containing an Initial Flaw*, Lehigh University, Bethlehem, 1974.
15. Milović, Lj., Vuherer, T., Radaković, Z., Petrovski, B., Janković, M., Zrilić, M., Daničić, D., *Determination of Fatigue Crack Growth Parameters in Welded Joint of HSLA Steel*, Structural Integrity and Life, 11 (3), 2011, pp.183-187.
16. Maneski, T., Milošević-Mitić, V., Ostrić, D., Postavke čvrstoće konstrukcija, Monografija, Mašinski fakultet Beograd, 2002.
17. Maneski, T., Milošević-Mitić, V., *Numerical and experimental diagnostics of structural strength*, Structural Integrity and Life, 10 (1), 2010, pp.3-10.